Isothermal and Nonisothermal Crystallization Kinetics of Poly(ϵ-Caprolactone)

Prarthana U. Dhanvijay,[1] Vikrant V. Shertukde,[1] Arun K. Kalkar[2]

[1]*Polymer Engineering and Technology Department, Institute of Chemical Technology, Nathalal Parekh Marg, Matunga(E), Mumbai 400019, India*
[2]*Department of Physics, Institute of Chemical Technology, Nathalal Parekh Marg, Matunga(E), Mumbai 400019, India*

Received 17 March 2010; accepted 8 January 2011
DOI 10.1002/app.34045
Published online 18 October 2011 in Wiley Online Library (wileyonlinelibrary.com).

ABSTRACT: With increasing environmental awareness, evaluating the potential of biopolymers as a substitute for traditional materials has been of great interest. Crystallization kinetics provides fundamental knowledge required for evaluation, playing vital role in determining the final properties of the product. In this study, the isothermal and nonisothermal crystallization kinetics of poly(ε-caprolactone) (PCL) were investigated with the help of various models. The Avrami model best described the isothermal crystallization kinetics, suggesting three-dimensional spherulitic growth, which was in agreement with the morphology studies; whereas the Liu model fit well under nonisothermal crystallization conditions. The failure of the Kissinger model to determine the activation energy was overcome with the Friedman model. The kinetic crystallizability determined by the Ziabacki model indicated a higher crystallization ability of PCL at lower cooling rates. © 2011 Wiley Periodicals, Inc. J Appl Polym Sci 124: 1333–1343, 2012

Key words: biopolymers; crystallization; morphology

INTRODUCTION

The crystallization process significantly influences polymer properties through the crystal structure and morphology established during the phase transition from the viscous molten state to the semicrystalline solid state. In the conventional melt processing of polymers, the crystallization behavior and kinetics provide insight into the underlying molecular processes and the resulting morphology. Crystallization from the melt proceeds at a finite rate under nonequilibrium conditions after a process of nucleation and crystal growth until a pseudo-equilibrium of crystallinity is achieved.[1] In practical processing, crystallization usually proceeds under isothermal and nonisothermal conditions. Therefore, kinetic crystallization treatments can be used to elucidate the mechanism of nucleation and growth in polymeric crystals, which is, without doubt, of great theoretical interest. Isothermal crystallization measurements are usually used to study the crystallization behavior of polymers because their theoretical analysis is relatively easy.[2] The treatment of nonisothermal crystallization data, in which the samples are observed at a constant cooling rate (λ), is theoretically more complicated,[3] although very important, because this type of crystallization approaches more closely the industrial conditions of polymer processing. To control the rate of crystallization ($\tau_{1/2}$) and the degree of crystallinity and obtain materials with better physical properties, a great deal of effort has been devoted to studying crystallization kinetics with the help of various mathematical models and determining the change in material properties.[4]

The crystallization behavior[4,5] and kinetics of polymeric materials have been reviewed previously.[6–8] In particular, the isothermal and nonisothermal crystallization kinetics of commodity and engineering polymers, such as isotactic polypropylene,[9–12] filled polypropylenes,[13,14] poly(ethylene terephthalate),[15,16] poly(trimethylene terephthalate),[17,18] poly(butylenes terephthalate),[19] nylon,[20–22] and poly(sulfides),[23–25] have been investigated in detail, and to much lesser extent, those of biopolymers, such as poly(lactic acid)[26–29] and poly(ε-caprolactone) (PCL),[30–33] have been studied, although they have found wide commercial importance.

Biodegradable PCL is an aliphatic polyester with semicrystalline characteristics. PCL can be degraded by hydrolysis of its ester linkages alone in the polymer chains in physiological conditions and has, therefore, found a wide range of possible applications, such as biodegradable packaging materials, implantable biomaterials, and microparticles for drug

Correspondence to: V. V. Shertukde (vikrantsher@rediffmail.com).

delivery. Many researchers have attempted to study the crystallization behavior of PCL; however, to our knowledge, in almost all of the reported literature, studies on the crystallization kinetics and morphology of pure unblended PCL exists only as a part of copolymers,[34–37] blends,[38–45] and composites.[46–49] Moreover, the research has mostly been aimed at evaluating the isothermal crystallization kinetics and growth rate phenomena. In this study, an effort was made to extend the crystallization kinetics study to nonisothermal conditions also, as common industrial processes usually occur under these realistic circumstances, and to validate the findings over a wide range of mathematical models, as this may provide insight into understanding the isothermal and nonisothermal crystallization kinetics of PCL. On the basis of the results obtained, a comparative analysis between different models was also performed.

EXPERIMENTAL

Specimens

The PCL used in this study was supplied by Solvay Caprolactones Ltd, Warrington, United Kingdom and had a melt flow index value of 40 g/10 min, a weight-average molecular weight (M_w) of 43,000, a number-average molecular weight (M_n) of 28,000, and a polydispersity of 1.52 as, determined by high-performance liquid chromatography with polystyrene as a calibration standard. The samples were dried in an air-circulating oven at 40°C for 6 h before use to remove any residual moisture within the sample. To prepare films for further characterization, a solvent casting method was used. The material was allowed to dissolve in tetrahydrofuran solvent for 3 h with continuous stirring. The solution was then transferred to the vacuum oven maintained at 35°C and kept there for 24 h.

Thermal analysis

The isothermal and nonisothermal crystallization kinetics were studied with a TA Q100 differential scanning calorimeter in a dry nitrogen atmosphere. The apparatus was calibrated with indium standards. The weight of the sample was kept constant at 8 mg for all measurements. For isothermal investigation, the samples were initially heated at 10°C/min from −20 to 90°C and held there for 5 min to eliminate any previous thermal history. Then, the samples were cooled at 65°C/min to a range of crystallization temperatures (T_c's), 38, 40, 42, 44, and 46°C, where they were kept for 60 min to promote isothermal crystallization, and the curves for heat flow as a function of time were recorded for each isothermal T_c. The nonisothermal crystallization was set to study the formation of crystallites in PCL, depending on different λ's. The samples were heated to 90 and 30°C above the melting temperature (T_m) of PCL, at 5, 10, 15, 20, 25, and 30°C/min and held there for 5 min to eliminate residual crystals in the melt. The melt was then cooled to −20°C, and the exothermic curves of heat flow as a function of both the time and temperature were recorded for each λ. Although Pijpers et al.[50] suggested the use of high-speed, high-performance DSC for the study of the kinetics and metastability of macromolecular systems, it is appreciable for very high heating rates and λ's. Because the heating and cooling scans used in this study fell well within the efficiency of the instrument and also as the mass compensation was done, the data obtained could be useful in determining the crystallization kinetics both isothermally and nonisothermally.

Structural analysis

Optical microscopy was performed with an Olympus polarizing optical microscope equipped with a cross-polar and a Mettler hot stage. The sample thickness for the observation was about 2 μm. The crystallization process was examined with the following temperature sequence. The polymer was heated on a hot stage to 90°C, which was 30°C above the melting point of PCL. It was then kept for 15 min to eliminate any previous thermal history, and then, it was allowed to cool gradually up to room temperature. The spherulitic morphology was monitored between the crossed polarizer and recorded at appropriate time intervals by a digital camera mounted on the microscope. The crystal growth was observed at the proposed T_c's of 44, 46, and 48°C, where it was kept for 1 h.

RESULTS AND DISCUSSION

Isothermal crystallization

The isothermal crystallization behavior of PCL was determined from the plot of the relative degree of crystallinity [$X(t)$] versus time (minutes), as shown in Figure 1. This curve shifted to the right with increasing T_c; this suggested that with the increase in T_c's, the temperature gradient decreased markedly to the point where sample could not undergo quenching. However, as T_c was decreased and the sample reached the desired temperature, the onset time of crystallization decreased accordingly. The sample was effectively quenched when cooled; thus, crystallization occurred rapidly over a much shorter timescale. The crystallization exotherm also became much sharper as T_c was decreased because of the increased $\tau_{1/2}$, a consequence of the larger temperature gradient between T_m and T_c.

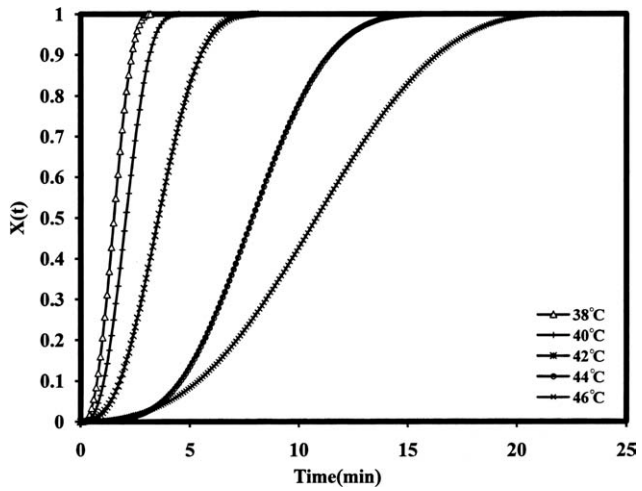

Figure 1 $X(t)$ versus time for isothermal crystallization.

Avrami model for isothermal crystallization

The crystallization process itself is strongly temperature dependent and is usually treated as a composite of two stages: primary and secondary crystallization. With the assumption that $X(t)$ increases with an increase in crystallization time (t), the Avrami[51–53] equation could be used to analyze the isothermal crystallization process of PCL as a function of t, as described in eq. (1):

$$X(t) = 1 - \exp(-Kt^n) \quad (1)$$

where $X(t)$ is the relative degree of crystallinity obtained with the least squares method, which integrates each of the crystallization curves at a set interval of time, between the onset and offset times; K is the reaction rate parameter; and n is the Avrami exponent, which determines the crystal geometry and nucleation type. A double-logarithmic plot of $\log\{\ln[1 - X(t)]\}$ versus $\log t$ was produced to obtain n (from the slope) and K (from the intercept), as shown in Figure 2. The Avrami plot shows mostly

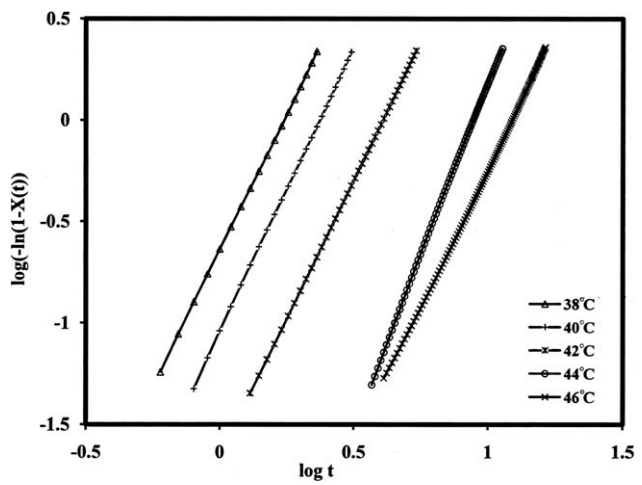

Figure 2 Avrami plots for isothermal crystallization.

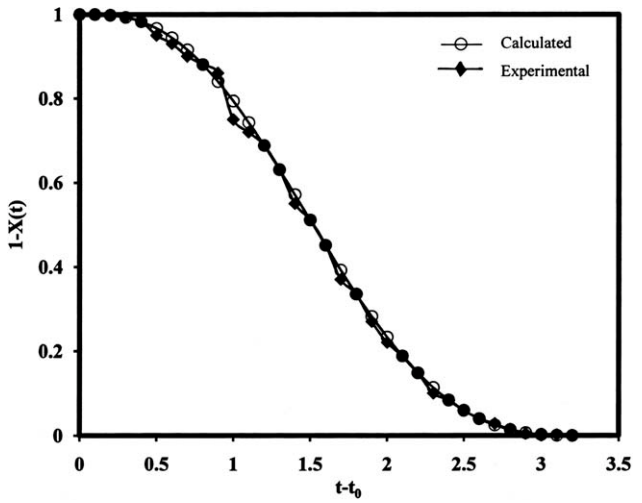

Figure 3 Superposition of the experimental and calculated amounts of uncrystallized material as a function of time for PCL at 38°C.

linear characteristics, justifying that the Avrami equation best described the isothermal crystallization kinetics of PCL. All lines were almost straight and parallel to each other, shifting to a higher time with increasing temperature. However, this linear characteristic subsequently tended to level off, creating a possibility for the existence of a secondary crystallization stage if the entire crystallization range is considered. So the fit to eq. (1) was performed in the range 1–80% (i.e., in the entire primary crystallization range), where correlation coefficients of 0.9999 were obtained. Also, to avoid any error while estimating various parameters, we prepared plots that compared the experimental and calculated curves of the unconverted PCL fraction to evaluate the quality of the fit, as depicted in Figure 3. The values of n and K determined from the slope and intercept of the initial linear portion of the plots in Figure 2 are listed in Table I. n was in the range from 2.6 to 3.4; this indicated a three-dimensional heterogeneous nucleation with a spherical crystal geometry, which was in good agreement with the values of 2.5–3.5 reported by Goulet and Prud'homme[54] for temperatures ranging from 40 to 49°C for $M_w = 48{,}000$ and the n values of 2.2–2.8 published by Priftis et al.[55] for $M_n = 29{,}000$ in a temperature range of 42–48°C. Skoglund and Fransson[56] found an n value of 3 for $M_w = 55{,}000$ at 47°C, whereas Balsamo et al.[57] reported n values between 3 and 3.7 in a 35–48°C temperature range for a similar molecular weight PCL. The Avrami index for the PCL homopolymer was confirmed as 3 by Muller et al.[58]

Table I also lists other important parameters for this analysis, including the half-time of crystallization ($t_{1/2}$), which is defined as the time taken from the onset of crystallization until 50% completion, which was determined from Figure 1.

TABLE I
Isothermal Parameters for PCL Determined from the DSC Curve

Temperature (°C)	$t_{1/2(\text{experimental})}$ (min)	$t_{1/2(\text{calculated})}$ (min)	$\tau_{1/2}$ (min^{-1})	$t_{\max}$ (min)	n	$1/T_c$	$1/n \ln K$	K (min^{-n})
38	1.50	1.52	0.65	1.46	2.67	0.026	−0.25	0.225
40	2.12	2.06	0.48	2.01	2.79	0.025	−0.14	0.0911
42	3.61	3.56	0.28	3.44	2.73	0.023	−0.09	0.0216
44	7.90	7.91	0.12	7.95	3.40	0.022	−0.03	0.0006
46	10.9	10.75	0.09	10.41	2.73	0.021	−0.05	0.0001

The relationship between the K and $t_{1/2}$ is as follows:

$$t_{1/2} = \left(\frac{\ln 2}{K}\right)^{1/n} \tag{2}$$

The dependence of $t_{1/2}$ obtained experimentally and that calculated with eq. (2) with T_c is shown in Figure 4, and as is the case for all polymeric materials, $t_{1/2}$ increased with increasing T_c for a relatively lower degree of supercooling.

Usually, $\tau_{1/2}$ is described as the reciprocal of $t_{1/2}$; these values were used to calculate the time required for the maximum crystallization rate ($t_{\max}$) because this time corresponded to the point where the rate of change of heat flow with time was equal to zero, as given by

$$t_{\max} = \left(\frac{n-1}{nK}\right)^{1/n} \tag{3}$$

The values of $t_{\max}$ determined are listed in Table I.

As seen from Table I, with increase in T_c, the Avrami rate constant (Z_t) decreased; this was evident from the literature published.[59] This suggests that at low T_c's, the high degree of undercooling overcame the energy barrier quickly and easily contributed toward less time and faster crystallization.

Activation energy for crystallization

If the crystallization process is assumed to be thermally activated, K can be approximately described by an Arrhenius-type equation as reported by Cebe and Hong:[60]

$$K^{1/n} = k_0 \exp -\left(\frac{\Delta E}{RT_c}\right) \tag{4}$$

where k_0 is the pre-exponential factor or simply the *prefactor*. The units of the pre-exponential factor are identical to those of the rate constant and will vary depending on the order of the reaction; R is the universal gas constant; the Kissinger activation energy (ΔE) can be determined by the slope of a plot of $1/n(\ln K)$ versus $1/T_c$ and the value of ΔE for PCL was found to be −223.7 kJ/mol. As the polymer had to release energy while transforming from the melt to the crystalline state, the value of ΔE was negative. Also, as the activation energy for crystallization is very temperature dependent, extrapolation above the measured boundaries was not possible. Chen and Wu[61] reported a somewhat higher activation energy value of −333.8 kJ/mol for PCL with an M_n of 42,000; this may have been due to the difference in M_n.

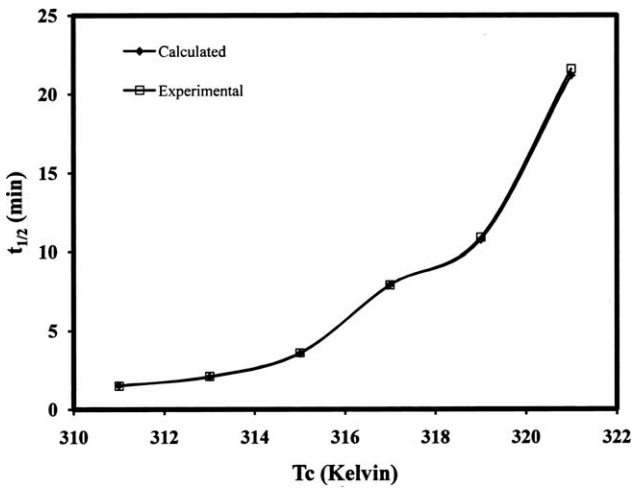

Figure 4 Plot of $t_{1/2}$ versus T_c.

Nonisothermal crystallization

From the DSC curves of samples crystallized from the melt state at a given λ, some useful parameters can be obtained to describe the nonisothermal crystallization. These parameters include the peak T_c, which is the temperature at which the value of the heat flow is maximum; the temperature at the intercept of the tangents at the baseline and the high-temperature side of the exotherm (T_{con}); and the end temperature of crystallization (T_{coff}). All of these parameters were determined from the typical DSC curves of heat flow as a function of the temperature at various λ's, as shown in Figure 5, and the results are depicted in Table II.

When λ was increased, this caused T_{con}, T_{coff}, and T_c to shift to lower temperatures. Conversely, this caused the time taken to reach onset, peak, and offset T_c's to decrease. This implied that lower the λ was, the earlier crystallization started. From the DSC cooling cycle, information on the values of the relative crystallinity as a function of both temperature and time were determined. The percentage crystallinity of the sample [$X(T)$] was calculated by the integration of the crystallization exotherms with the

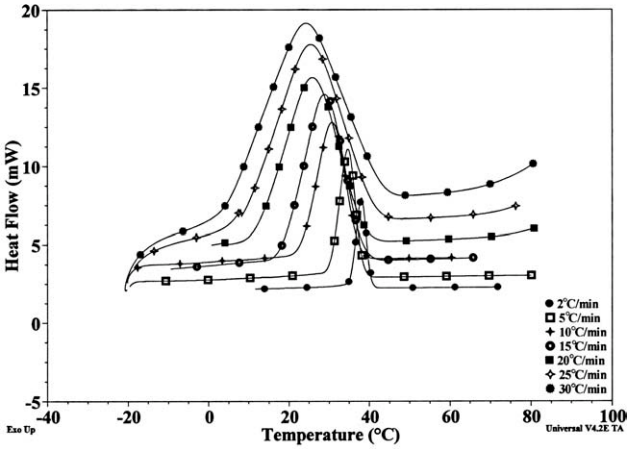

Figure 5 Schematic representation of all of the parameters of crystallization during the nonisothermal crystallization process.

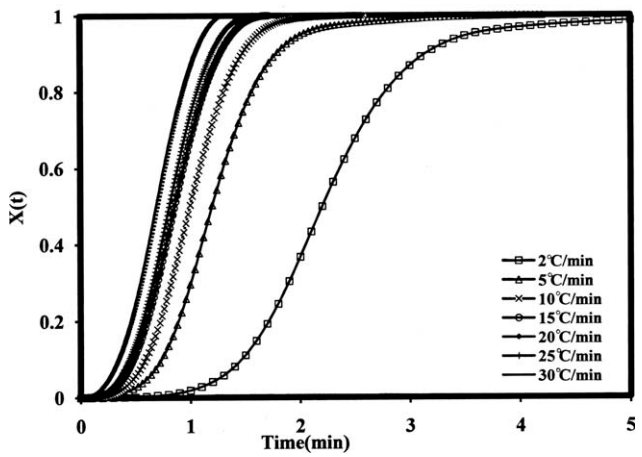

Figure 6 Change of $X(t)$ as a function of time.

least squares method at specific intervals of temperature. $X(T)$ was then obtained with the quotient of the total number of squares under the curve and the number of squares between T_{con} and the specified temperature for that λ. Therefore, a range of values of $X(T)$ between T_{con} and T_{coff} for each λ was converted to $X(t)$ (see Fig. 6). A similar plot was found when a graph of $X(T)$ versus temperature was produced and is shown in Figure 7, and for both Figures 6 and 7, a series of S-shaped curves were obtained. In the primary crystallization region, that is, below $X(T) = 0.8$, $\tau_{1/2}$ was high, as shown by the steepness of the gradient of the curve in this region. Above $X(T) = 0.8$, $\tau_{1/2}$ then slowed, and the curve reached a plateau, with the curves finally having a distinctive sigmoidal (S) shape. At higher λ's, the transition between the primary and secondary crystallization regions was less pronounced; however, it was clear that there was a change in the crystallization rate. This change in rate was attributed to spherulite impingement, as previously described by Wunderlich[1] and Poisson.[3] They reported the primary growth stage to continue unrestricted until a point where the individual crystals begin to touch and, therefore, restrict their rate of growth.

To more accurately describe the mechanism of the stages of crystallization experienced by PCL, a number of models have been developed to describe the nonisothermal crystallization kinetics of polymers. Their applicability to the PCL used in this study was investigated with models such as the Jeziorny-modified Avrami, Ozawa, Liu, ΔE, Friedman, and Ziabicki models.

Jeziorny-modified Avrami model

The analysis of the time-dependent relative crystallinity function, $X(t)$, for nonisothermal crystallization was carried out with the modified Avrami equation, which can be written as follows:

$$X(t) = 1 - \exp(-Z_t t^n) \tag{5}$$

where n is a mechanism constant that depends on the type of nucleation and growth process and Z_t is the Avrami rate constant, involving nucleation and growth parameters. Because the process is nonisothermal, Jeziorny[62] suggested that Z_t should be corrected for the influence of λ of the polymer. When λ is assumed to be constant or approximately constant, the final form of the parameter characterizing the kinetics of nonisothermal crystallization is given as follows:

TABLE II
Nonisothermal Parameters for PCL Determined from the DSC Curve

λ (°C/min)	T_{con} (°C)	T_{coff} (°C)	T_{cmax} (°C)	t_{on} (min)	t_{off} (min)	t_{max} (min)	X_c (%)	ΔH_c (mW)
2	40	29.03	38.02	82	93	86.97	50.25	68.34
5	38.18	29.93	34.7	36	44	39.13	44.88	61.04
10	37.14	20.23	30.75	21	25	23	41.66	55.65
15	38.23	18.57	28.89	16	18.7	17.48	46.62	63.4
20	38.45	12.23	25.85	13.5	15	14.47	45.27	61.57
25	41.1	8.48	25.49	12	14	13.06	46.15	62.77
30	43.45	4.03	24.22	11	13	11.94	50.95	69.3

T_{cmax}, peak crystallization temperature; t_{on}, onset time; t_{off}, offset time; X_c, percent crystallinity; and ΔH_c, entalpy of crystallization.

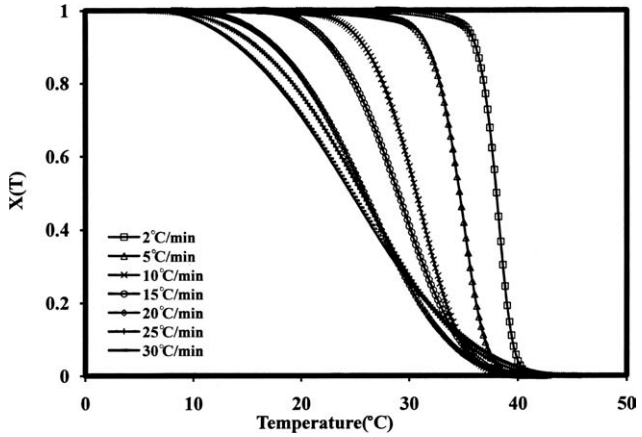

Figure 7 Change of $X(t)$ as a function of temperature.

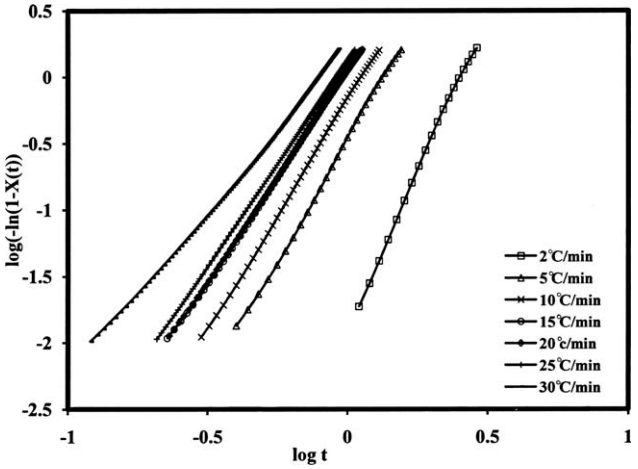

Figure 8 Avrami plot for PCL.

$$\ln Z_c = \frac{\ln Z_t}{\lambda} \tag{6}$$

where Z_c is the rate parameter with respect to cooling rate.

If the double-logarithmic plot of eq. (5) adequately describes the nonisothermal crystallization behavior of a polymer, the plot of $\log\{-\ln[1 - X(t)]\}$ versus $\log t$ would be straight lines, and one should be able to obtain the values of n and Z_t from the slopes and intercepts, respectively. The Jeziorny-modified Avrami plot for PCL is shown in Figure 8. From this figure, it was evident that the linearity of the plots was poor; this indicated the existence of a two-stage crystallization process for PCL, and the crystallization process could be divided into primary and secondary stages. The values of n, Z_t, and Z_c for both stages are listed in Table III. At the primary stage of crystallization, n_1 decreased from 4.7 to 2.5 with increasing λ; this closely resembled the findings of Wu and Chen,[63] with n values between 4.3 and 3.5, and Wu et al.,[64] who suggested average n value of 4 for pure PCL. This trend showed that more crystal perfection was achieved at lower λ values because low λ's provide more fluidity, more diffusivity, and, especially, more time at high temperatures for perfect crystallization. n corresponding to the primary stage of crystallization was essentially greater than 2, which revealed that the PCL polymer chains were apt to take three-dimensional crystallization growth with heterogeneous athermal nucleation. In common, at the secondary stage, the form of spherulites growth transformed into the lower dimensional space extension, and the corresponding n_2 values ranged from 1.4 to 2.6. This was attributed to the effect of slower crystallization or the further perfection of crystal caused by spherulitic impingement or to the reorganization of initially poorly crystallized macromolecules or small and metastable crystals.

Ozawa model

Generally, the Ozawa theory[65] has been used to describe the nonisothermal crystallization kinetics of polymers and is based on Avrami theory. Ozawa modified the Avrami equation for nonisothermal treatment, assuming that the polymer melt was cooled at a constant rate. According to Ozawa theory, the degree of conversion or $X(T)$ at temperature T could be calculated as follows:

$$1 - X(T) = \exp\left[\frac{-k(T)}{\lambda^m}\right] \tag{7}$$

where m is the Ozawa exponent, which depends on the dimension of crystal growth, and k is the cooling

TABLE III
Avrami Parameters for the Crystallization of PCL

λ (°C/min)	$t_{1/2}$ (min)	n_1	n_2	Z_{t1}	Z_{c1}	Z_{t2}	Z_{c2}
2	2.2	4.73	1.49	0.01	0.006	0.39	0.197
5	1.2	3.66	1.51	0.34	0.068	0.97	0.195
10	1.0	3.48	2.77	0.67	0.067	0.78	0.078
15	0.87	3.19	2.28	1.11	0.074	1.06	0.070
20	0.85	3.17	2.37	1.11	0.055	1.04	0.052
25	0.83	3.10	2.44	1.32	0.053	1.26	0.050
30	0.70	2.53	2.64	1.78	0.059	2.07	0.069

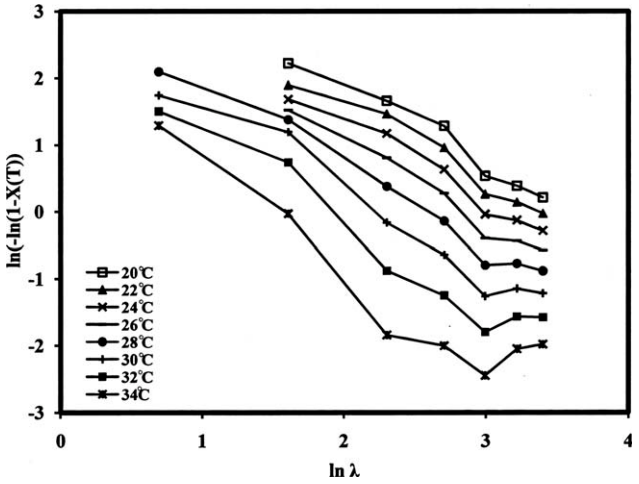

Figure 9 Ozawa plot for PCL.

crystallization function, which is related to overall crystallization rate and indicates how fast crystallization occurs.

Equation (7) can be written as

$$\ln\{-\ln[1 - X(T)]\} = \ln k(T) - m \ln \lambda \tag{8}$$

From the plots of ln}−ln[1 − $X(T)$]} against ln λ, the kinetic parameters $k(T)$ and m should be obtainable from the intercepts and slopes of the lines, respectively. A graph for Ozawa theory was constructed from the data points taken at different temperatures in the range 22–34°C during the crystallization process and is shown in Figure 9. The Ozawa plot shows nonlinearity over the entire temperature range considered and indicates a failure to provide an adequate description of the crystallization of PCL. This was also confirmed from the values of regression coefficients, which were below 0.9. In Ozawa analysis, comparison is to be carried out on the experimental data representing widely varying physical states of the system[66]; however, these differences have not been taken into account in the model. Thus, if the λ's vary in the range and if a large amount of crystallization occurs as a result of secondary processes, the Ozawa model would not be adequate in describing the nonisothermal crystallization behavior because Ozawa assumed a negligible effect of secondary crystallization. Because we observed a breakdown of the Ozawa model, we did not further analyze the data in the context of this model to extract m or the crystallization rate parameter.

Liu model

From the previous analysis, it was evident that the modified Avrami and Ozawa approaches did not consider the importance of secondary crystallization and so less satisfactorily described the behavior of PCL. So, attempts were made to modify and combine these two basic approaches to study the nonisothermal crystallization behavior of polymers. In one such attempt, Liu et al.[67] suggested a convenient procedure for characterizing nonisothermal crystallization kinetics by combining the Avrami and Ozawa equations on the basis of the assumption that the degree of crystallinity is corrected to λ and t (or temperature T). Therefore, their relationship for nonisothermal crystallization could be derived by the combination of eqs. (9) and (10) as follows:

$$\ln K + n \ln t = \ln k(T) - m \ln \lambda \tag{9}$$

$$\ln \lambda = \ln F(T) - b \ln t \tag{10}$$

where the parameter $F(T) = \left[\frac{k(T)}{K}\right]^{1/m}$ refers to the necessary value of λ to reach a defined degree of crystallinity at unit t and b is the ratio between n and m, that is, $b = n/m$. Nonisothermal crystallization is difficult to describe with a single equation because there are a lot of parameters that have to be taken into account simultaneously. The importance of this method is that it correlates λ with the temperature, time, and morphology. From eq. (10), it follows that at a given degree of crystallinity (here for 10, 20, 30, 40, 50, 60, 70, 80, and 90%), a plot of ln λ against ln t was obtained, which is shown in Figure 10. The values of b and $F(T)$ for a certain value of $X(t)$ were determined from the slope and intercept of the best fit trend line drawn through the data points for each λ at the assigned value of $X(t)$. The data for Liu's analysis is shown in Table IV. It was evident from Figure 10 and Table IV that there was good agreement between the Liu analysis and the experimental data for PCL, as the values of the coefficient of determination for trend lines (R^2) were in excess of 0.95 for each plot at the assigned value of $X(t)$. In agreement with that reported by Liu, the values of $F(T)$ systematically increased with rising

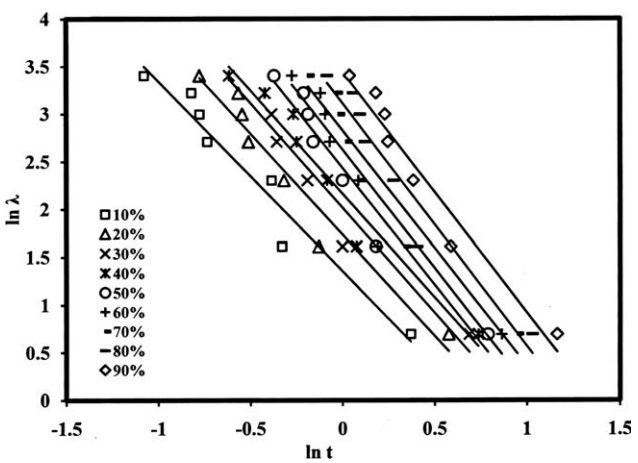

Figure 10 Combined Avrami/Ozawa plots for PCL.

TABLE IV
Values of *b* and *F(T)* as a Function of *X(t)*

X(t) (%)	*b*	ln *F(T)*	*F(T)*	R^2
10	1.983	1.352	3.866	0.9503
20	2.117	1.733	5.657	0.9661
30	2.196	2.016	7.509	0.9633
40	2.116	2.163	8.698	0.9537
50	2.447	2.433	11.400	0.9777
60	2.482	2.625	13.805	0.9562
70	2.467	2.824	16.855	0.9586
80	2.546	3.111	22.452	0.9652
90	2.523	3.440	31.202	0.9514

relative crystallinity; this indicated that at a unit t, a higher λ should be used to obtain a higher degree of crystallinity. Liu, Mo, et al.[68] stated that the values of b remained almost constant, independent of the value of $X(t)$. However, the values listed in Table IV showed a small increasing trend as the value of $X(t)$ increased. This change in the exponent b was determined by the time taken for crystallization to reach completion. In Figure 10, it can be seen that the slower λ's resulted in a longer time over which crystallization occurred; conversely, increasing λ reduced the time of crystallization.

ΔE

Accounting for the influence of various λ's in the nonisothermal crystallization process, Kissinger[69] reported that the activation energy could be determined on the basis of the following equation:

$$k_t = A \exp\left[\frac{-E}{RT}\right] \tag{11}$$

where A is the pre-exponential factor or simply the prefactor.

As the temperature changes, so does $\tau_{1/2}$; the maximum value of the reaction rate during crystallization occurs at T_c, and the derivative at that point with respect to time is zero. Kissinger, therefore, determined the activation energy (ΔE) with the following equation:

$$A \exp\left[\frac{-E}{RT_c}\right] = \frac{E}{RT_c^2}\frac{dT}{dt} \tag{12}$$

which can be rewritten as

$$\frac{d\left[\ln\left(\frac{\lambda}{T_c^2}\right)\right]}{d\left(\frac{1}{T_c}\right)} = -\frac{\Delta E}{R} \tag{13}$$

$\Delta E/R$ was determined from the slope of the best fit trend line of λ/T_c^2 versus $1/T_c$ plot. As the polymer has to release energy while transforming from the melt to the crystalline state, the value of ΔE is negative on the basis of the concept of heat quantity in physical chemistry. The individual values of $1/T_c$ dependent on λ were found to show good agreement in this study. ΔE for the nonisothermal crystallization of PCL was found to be 148.9 kJ/mol, which satisfactorily agreed with the literature.[63] It is noted that the ΔE obtained from the nonisothermal crystallization was smaller than those obtained from the isothermal crystallization (333.8 kJ/mol). This indicated that the dominant factor of crystalline formation in PCL was changed from the crystal growth mechanism of isothermal crystallization into the nucleation mechanism of nonisothermal crystallization.

Friedman analysis

Because the Kissinger's procedure to obtain ΔE was formulated for only heating experiments (i.e., positive values of λ), the differential isoconversional methods of Friedman[70] were the most appropriate for the investigation of the effective activation energy.

The Friedman equation is expressed as follows:

$$\ln\left(\frac{dX}{dt}\right)_{X,i} = \text{Constant} - \frac{\Delta E_x}{RT_{x,i}} \tag{14}$$

where dX/dt is the instantaneous crystallization rate as a function of temperature at a given conversion (X). According to this method, the $X(t)$ function obtained from the integration of the experimentally measured crystallization rates is initially differentiated with respect to time to obtain the instantaneous crystallization rate (dX/dt). Furthermore, by selecting appropriate degrees of crystallinity (i.e., from 5 to 95%), the values of dX/dt at a specific X were correlated to the corresponding T_c at this X, that is, T_x. Then, when the left-hand side of eq. (14) is plotted against $1/T_x$, a straight line must be obtained with the slope equal to $\Delta Ex/R$; the respective data is given in Table V. As the isoconversional method accounts for the temperature program in its most

TABLE V
Data Determined from the Friedman Analysis

Crystallinity (%)	Temperature range (K)	R^2	Activation energy (kJ/mol)
5	307–312	0.9	1128.54
10	307–312	0.93	996.34
20	304–312	0.93	737.78
30	301–311	0.91	536.50
40	300–311	0.93	496.01
50	297–312	0.95	381.36
60	295–311	0.94	394.66
70	293–311	0.95	392.58
80	290–310	0.93	356.08
90	287–309	0.96	457.76

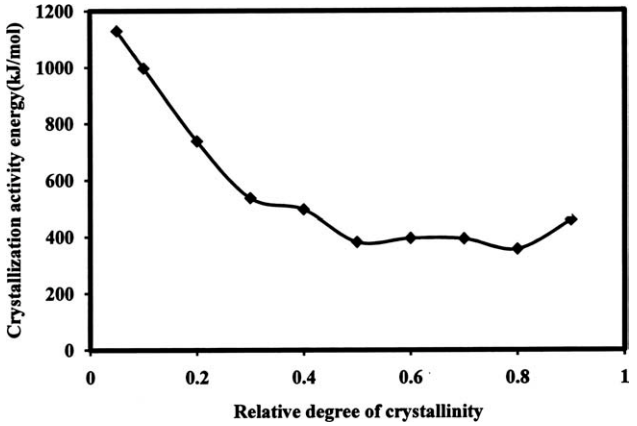

Figure 11 Plot of $X(t)$ versus crystallization activity energy.

general mathematical form, T_x, and imposes no limitations; so it can be used for heating as well as for cooling. Apart from this, it also permits the estimation of effective activation energies for a complex process whose temperature dependence of the overall rate cannot be described by a single Arrhenius equation over a wide temperature range. The evaluation of the effective activation energy as a function of the extent of X has the additional benefit of detecting changes in the process mechanism that are likely to occur in such a complex process as polymer crystallization. Figure 11 shows that the crystallization activation energy takes large values at a lower extent of X, which corresponds to the melting point; then becomes stable; and then increases again. This shows that with the start of the crystallization process, to achieve the slightest X initially, a higher amount of energy is required for the transport of molecular segments to the crystallization surface.

Ziabicki analysis

Ziabicki[71,72] developed a theory based on the assumption that crystallization can be presented by means of the equation for first-order kinetics, where the crystallization rate constant [$K(T)$] is only temperature-dependent.

$$\frac{dX}{dt} = [1 - X]K(T) \tag{15}$$

The change of $K(T)$ as a function of temperature is illustrated by a curve resembling a Gaussian curve. Here, for a given λ, the changes in $K(T)$ as a function of the temperature can be described by a Gaussian function of the following form:

$$K(T) \approx K_{\max} \exp\left\{-4 \ln 2[(T - T_{\max})^2/D^2]\right\} \tag{16}$$

where $K_{\max}$ is the maximum value of the rate corresponding to $T_{\max}$, D is the half-width of the crystallization curve, and $T_{\max}$ is the temperature at which the crystallization rate is at a maximum. With the isokinetic approximation integration method over a crystallization range of temperatures ($T_g < T < T_m$) for a given λ, the equation enables one to calculate the characteristic quantity understood as the kinetic crystallizability (G):

$$G = \int_{T_g}^{T_{\max}} K(T)dT = (\pi/\ln 2)^{1/2} K_{\max} D/2 \tag{17}$$

where G is the parameter characterizing the kinetics of the nonisothermal crystallization process and represents the degree of crystallinity transformation when the polymer is cooled at a unit arbitrary cooling rate (ϕ) from T_m to T_g. In the case of a nonisothermal crystallization process where λ is changing, $K(T)$ is replaced with a derivation function of the relative crystallinity, $(dX/dt)\phi$, which is specific for each λ. Therefore, the equation is replaced by

$$G_\varphi = \int_{T_g}^{T_{\max}} \left(\frac{dX}{dt}\right)_\varphi = \left(\frac{\pi}{\ln 2}\right)^{1/2} \left(\frac{dX}{dt}\right)_{\varphi,\max} \frac{D_\varphi}{2} \tag{18}$$

where $(dX/dt)_{\phi,\max}$ is the maximum crystallization rate and D_ϕ is the half-width of the derivative relative crystallinity as a function of dX/dt. G_ϕ is the kinetic crystallizability at ϕ, which again can be normal for ϕ by the division of G_ϕ by ϕ:

$$G_c = \frac{G_\varphi}{dT/dt} \tag{19}$$

where G_c represents the ability of a semicrystalline polymer to crystallize when it is cooled from the melt (T_m) to a glassy state (T_g) at ϕ. The calculation of the G_ϕ parameter was made possible by knowledge of the values of $(dX/dt)_{\phi,\max}$ and D_ϕ appearing in eq. (19). D_ϕ could be easily determined from the crystallization thermogram. The $(dX/dt)_{\phi,\max}$ value corresponding to $T_{\max}$, at which the crystallization rate is at a maximum, could be calculated, and these

TABLE VI
Values of the Parameters Obtained from the Ziabacki Analysis

λ (°C/min)	$T_{\max}$ (K)	$(dX/dt)_{\phi,\max}$	D_ϕ	G_ϕ	G_c
2	311.4	0.33	3.11	2.18	1.09
5	308.2	0.20	4.49	1.91	0.38
10	304.4	0.17	8.87	3.21	0.32
15	303	0.085	12.44	2.25	0.15
20	300	0.064	16.39	2.23	0.11
25	299.8	0.053	18.52	2.09	0.08
30	298.4	0.048	20.11	2.05	0.06

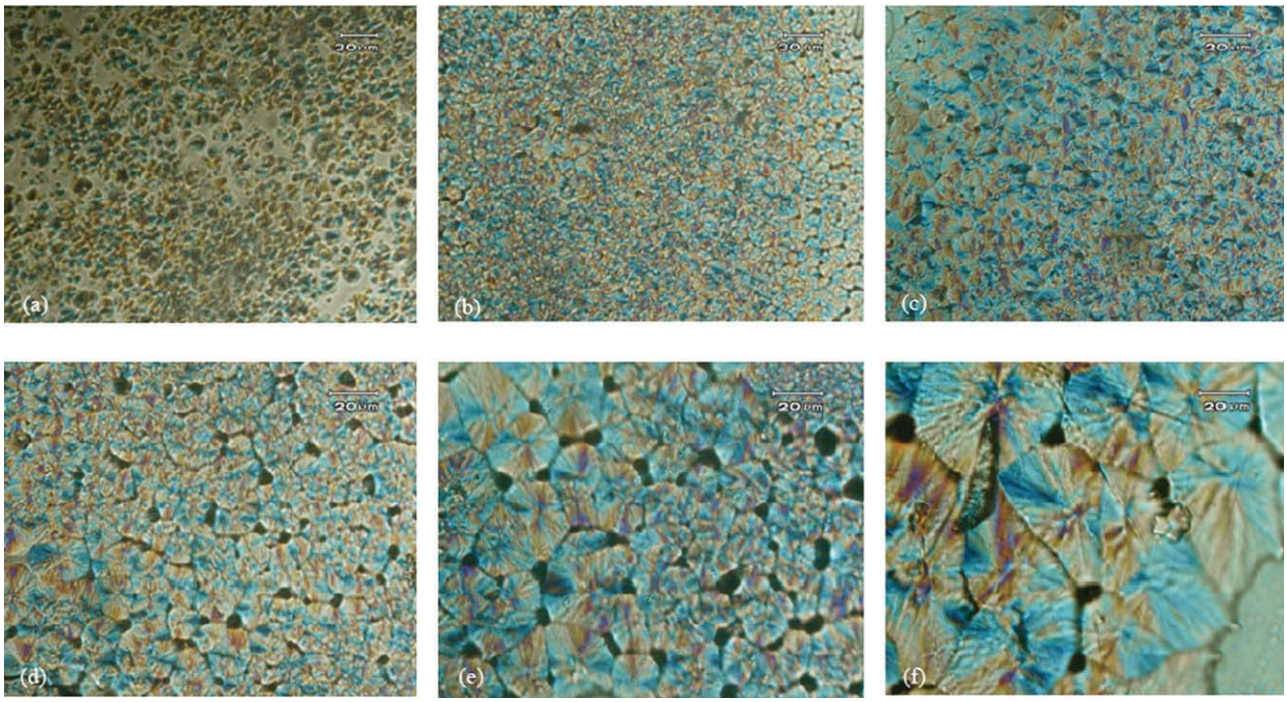

Figure 12 Optical micrographs between crossed polars for (a–c) gradual evolution of the spherulites with respect to time and T_c = (d) 44, (e) 46, and (f) 48°C. [Color figure can be viewed in the online issue, which is available at wileyonlinelibrary.com.]

values were then used to calculate G_c. The parameters characterizing G are listed in Table VI as follows.

It is evident from Table VI that D_ϕ showed an increasing trend with increasing λ; this suggested a broader crystal size distribution at higher λ's. Although the G_ϕ values dud not show any specific variation with respect to λ, when normalized for the effect of λ to obtain G_c, the kinetic crystallizability at ϕ suggested that G_c was a decreasing function of λ. The physical meaning of G is to characterize the ability of polymers in crystallizing when cooled from T_m toward the glass-transition temperature at ϕ. With higher G_c values, the polymer crystallized more readily; this indicated that at lower λ's, the crystallization ability of PCL was greater.

Morphology

As mentioned previously, morphology during isothermal crystallization was studied with a polarizing microscope and is shown in Figure 12. Figure 12(a–c) shows the gradual evolution of spherulites with respect to time, and Figure 12(d–f) shows spherulites formed during isothermal crystallization at proposed temperatures of 44, 46, and48°C.

It was observed from Figure 12 that when the melt was allowed to cool gradually to room temperature, initially, a large number of small nuclei appeared, increasing the crystalline density, which hindered the further growth of the crystals. However, when the crystallization was carried out isothermally at the proposed temperature, the evolution of crystals took place to a larger extent. With the increase in temperature, the thermal gradient decreased; this resulted in a large crystal size as seen in Figure 12(d–f).

CONCLUSIONS

A through investigation into the crystallization kinetics of PCL revealed that the Avrami model best described the isothermal crystallization kinetics and an indicative of existence of a secondary crystallization stage. n was in the range 2.5–3; this suggested a three-dimensional heterogeneous nucleation with a spherical crystal geometry. The decreased crystallization rate with increasing isothermal temperature was a result of an increase in the total t.

During nonisothermal crystallization, n_1 varied from 2.53–4.73 at the primary stage; this indicated that the mode of spherulitic nucleation and growth was more complicated than the isothermal process. However, because of the reduced crystallization rate during secondary crystallization, the spherulites grew in a lower dimensional space extension. Although the Ozawa model singly failed to describe the nonisothermal crystallization process, the combined Avrami and Ozawa equation modeled the process successfully. The lowering of the activation energy for the nonisothermal process (148.9 kJ/mol) as compared to the isothermal process (223.7 kJ/

mol) may have been due to a change in the mechanism. The Friedman model overcame the drawback of the Kissinger model for evaluating the activity energy and showed that with the onset of crystallization, a higher amount of energy was required to achieve the slightest X. The crystallization ability of PCL was greater at lower λ, as observed from the Ziabicki model data.

References

1. Wunderlich, B. Macromolecular Physics; Academic: New York, 1976; p 3.
2. Evans, U. R. Trans Faraday Soc 1945, 41, 365.
3. Poisson, S. D. Recherche sur la Probabilité des Jugements en matière criminelle et en matière civile; Bachelier: Paris, 1837.
4. Mears, P. Polymers: Structures and Properties; Van Nostrand: New York, 1965.
5. Bai, H.; Zhang, Y.; Zhang, Y.; Zhang, X.; Zhou, W. J Appl Polym Sci 2006, 101, 1295.
6. Lorenzo, M. L.; Silvestre, C. Prog Polym Sci 1999, 24, 917.
7. Lu, X. F.; Hay, J. N. Polymer 2001, 42, 9423.
8. Lorenzo, M. L. Prog Polym Sci 2003, 28, 663.
9. Wunderlich, B. Therm Acta 2003, 396, 33.
10. Long, Y.; Shanks, R. A.; Stachurski, Z. H. Prog Polym Sci 1995, 20, 651.
11. Carrubba, V.; Piccarolo, S.; Brucato, V. J Appl Polym Sci 2007, 104, 1358.
12. Martins, J. A.; Cruz Pinto, J. Polymer 2000, 41, 6875.
13. Bogoeva-Gaceva, G.; Janevski, A.; Gorzdanov, A. J Appl Polym Sci 1998, 67, 395.
14. Hammami, A.; Spruiell, J. E.; Mehrotra, A. K., Polym Eng Sci 1995, 35, 797.
15. Mubarak, Y.; Harkin-Jones, E. M. A.; Martin, P. J.; Ahmad, M. Polymer 2001, 42, 3171.
16. Wasiak, A. Polymer 2001, 42, 9025.
17. Tjong, S. C.; Xu, S. A. Polym Int 1997, 44, 95.
18. Li, J.; Zhou, C.; Gang, W. Polym Test 2003, 22, 217.
19. Sajkiewicz, P.; Carpaento, L.; Wasiak, A. Polymer 2001, 42, 5365.
20. Colomer Vilanova, P.; Montserrat Ribas, S.; Guzman, G. M. Polymer 1985, 26, 423.
21. Chuah, H. H. Polym Eng Sci 2001, 41, 308.
22. Apiwanthanakorn, N.; Supaphol, P.; Nithitanakul, M. Polym Test 2004, 23, 817.
23. Dangseeyun, N.; Srimohan, P.; Supaphol, P.; Nithitanakul, M. Therm Acta 2004, 409, 63.
24. McFerran, N. L. A.; Armstrong, C. G.; McNally, T. J Appl Polym Sci 2008, 110, 1043.
25. Liu, S.; Yu, Y.; Cui, Y.; Zhang, H.; Mo, Z. J Appl Polym Sci 1998, 70, 2371.
26. Wang, Y.; Liu, M.; Wang, Z.; Li, X.; Zhao, Q.; Fu, P. J Appl Polym Sci 2007, 104, 1415.
27. Minkova, L. I.; Magagnini, P. L. Polymer 1995, 36, 2059.
28. Lopez, L. C.; Wilkes, G. L. Polymer 1989, 30, 882.
29. Srinivas, S.; Babu, J. R.; Riffle, J. S.; Wilkes, G. L. Polym Eng Sci 1997, 37, 497.
30. Yasuniwa, M.; Tsubakihara, S.; Iura, K.; Ono, Y.; Dan, Y.; Takahashi, K. Polymer 2006, 47, 7554.
31. Yasuniwa, M.; Iura, K.; Dan, Y. Polymer 2007, 48, 5398.
32. Tsuji, H.; Takai, H.; Saha, S. Polymer 2006, 47, 3826.
33. Li, H.; Huneault, M. A. Polymer 2007, 48, 6855.
34. Shichun Jiang, S.; Ji, X.; An, L.; Jiang, B. Polymer 2001, 42, 3901.
35. Wang, J.; Dong, C. Polymer 2006, 47, 3218.
36. Xu, J.; Shi, W. Polymer 2006, 47, 5161.
37. Vincent, H.; Robert, E. Polymer 2005, 46, 7255.
38. Castillo, R. V.; Muller, A. J.; Raquez, J.; Dubois, P. Macromolecules 2010, 43, 4149.
39. Muller, A. J.; Albuerne, J.; Marquez, L.; Raquez, J.; Dege, P.; Dubois, P.; Hobbsc, J.; Hamleyd, I. Faraday Discuss 2005, 128, 231.
40. Hamley, I.; Parras, P.; Castelletto, V.; Castillo, R.; Muller, A.; Pollet, E.; Dubois, P.; Martin, C. Macromol Chem Phys 2006, 207, 941.
41. Nojima, S.; Ohguma, Y.; Kadena, K.; Ishizone, T.; Iwasaki, Y.; Yamaguchi, K. Macromolecules 2010, 43, 3916.
42. Lopez-Rodriguez, L.; Lopez-Arraiza, M., E.; Sarasua, J. R. Polym Eng Sci 2006, 46, 1299.
43. Senda, T.; He, Y.; Inoue, Y. Polym Int 2001, 51, 33.
44. Tsuji, H.; Yamada, T.; Suzuki, M.; Itsuno, S. Polym Int 2003, 52, 269.
45. Honma, T.; Senda, T.; Inoue, Y. Polym Int 2003, 52, 1839.
46. Balsamo, V.; Newman, D.; Gouveia, L.; Herrera, L.; Grimau, M.; Laredo, E. Polymer 2006, 47, 5810.
47. Balsamo, V.; Calzadilla, N.; Mora, G.; Muller, A. J Polym Sci Part B: Polym Phys 2001, 39, 771.
48. Lovera, D.; Marquez, L.; Balsamo, V.; Taddei, A.; Castelli, C.; Muller, A. Macromol Chem Phys 2007, 208, 924.
49. Qiu, Z.; Yang, W.; Ikehara, T.; Nishi, T. Polymer 2005, 46, 11814.
50. Pijpers, T. F. J.; Mathot, V. B. F.; Goderis, B.; Scherrenberg, R. L.; Vegte, E. W. Macromolecules 2002, 35, 3601.
51. Avrami, M. J Chem Phys 1939, 7, 1103.
52. Avrami, M. J Chem Phys 1940, 8, 212.
53. Avrami, M. J Chem Phys 1941, 9, 177.
54. Goulet, L.; Prud'homme, R. E. J Polym Sci Part B: Polym Phys 1990, 28, 2329.
55. Priftis, D.; Sakellariou, G.; Hadjichristidis, N.; Penott, E.; Lorenzo, A.; Muller, A. J Polym Sci Part A: Polym Chem 2009, 47, 4379.
56. Skoglund, P.; Fransson, A. J Appl Polym Sci 1996, 61, 2455.
57. Balsamo, V.; Calzadilla, N.; Mora, G.; Muller, A. J. J Polym Sci Part B: Polym Phys 2001, 39, 771.
58. Albuerne, J.; Marquez, L.; Muller, A. J.; Raquez, J. M.; Degee, P.; Dubois, P.; Castelletto, V.; Hamley, I. W. Macromolecules 2003, 36, 1633.
59. Jenkins, M. J.; Harrison, K. L. Polym Adv Technol 2006, 17, 474.
60. Cebe, P.; Hong, S. D. Polymer 1986, 27, 1183.
61. Chen, E.-C.; Wu, T.-M. Polym Degrad Stab 2007, 92, 1009.
62. Jeziorny, A. Polymer 1978, 19, 1142.
63. Wu, T.-M.; Chen, E.-C. Polym Eng Sci 2006, 1309.
64. Wu, T.; Zhang, X.; Yang, G. J Appl Polym Sci 2008, 107, 3796.
65. Ozawa, T. Polymer 1971, 12, 150.
66. Shangguan, Y. G.; Song, Y. H.; Zheng, Q. J Polym Sci Polym Phys 2006, 44, 795.
67. Liu, T.; Mo, Z.; Wang, S.; Zhang, H. Polym Eng Sci 1997, 37, 568.
68. Liu, S.; Yu, Y.; Cui, Y.; Zhang, H.; Mo, Z. J Appl Polym Sci 1998, 70, 2371.
69. Kissinger, H. E. J Res Natl Bur Stand (US) 1956, 57, 217.
70. Friedman, H. J Polym Sci Part C: Polym Symp 1964, 6, 183.
71. Ziabicki, A. Appl Polym Symp 1967, 6, 1.
72. Ziabacki, A. Polymer 1967, 12, 405.